

Word learning is mediated by the left arcuate fasciculus

Diana Lopez-Barroso^{1,2}, Marco Catani³, Pablo Ripollés^{1,2}, Flavio Dell'Acqua^{3,4,5}, Antoni Rodriguez-Fornells^{1,2,6} & Ruth de Diego-Balaguer^{1,2,6}

¹ Cognition and Brain Plasticity Group [Bellvitge Biomedical Research Institute]- IDIBELL, L'Hospitalet de Llobregat, Barcelona, 08097, Spain ² Dept. of Basic Psychology, Campus Bellvitge, University of Barcelona, L'Hospitalet de Llobregat, Barcelona 08097, Spain. ³ Natbrainlab, Department of Forensic and Neurodevelopmental Sciences, Institute of Psychiatry, King's College London, UK ⁴ Department of Neuroimaging, Institute of Psychiatry, King's College London, UK ⁵ NIHR Biomedical Research Centre for Mental Health at South London and Maudsley NHS Foundation Trust and King's College London, Institute of Psychiatry, UK ⁶ Catalan Institution for Research and Advanced Studies, ICREA, Barcelona, Spain

Submitted to Proceedings of the National Academy of Sciences of the United States of America

Human language requires constant learning of new words, leading to the acquisition of an average vocabulary of more than 30,000 words in adult life. The ability to learn new words is highly variable and may rely on the integration between auditory and motor information. Here, we combined diffusion imaging tractography and functional magnetic resonance imaging to study whether the strength of anatomical and functional connectivity between auditory and motor language networks is associated with word learning ability. Our results showed that performance in word learning correlates with microstructural properties and strength of functional connectivity of the direct connections between Broca's and Wernicke's territories in the left hemisphere. This study suggests that our ability to learn new words relies on an efficient and fast communication between temporal and frontal areas. The absence of these connections in other animals may explain the unique ability of learning words in humans.

arcuate fasciculus | functional connectivity | tractography | white matter | word learning

INTRODUCTION

Language is a unique human ability that has been suggested to depend on the evolution of direct connections between the temporal and frontal cortex for the integration of auditory and motor representation of words (1). Auditory-motor integration, involving the mapping of sound into articulation, has been proposed to be important not only for auditory perception (2) and speech processing (3, 4), but also for learning new words (1, 3, 5). The auditory-motor integration theory of speech is based in part on the observation that patients with lesions affecting the arcuate fasciculus (AF) connecting temporal and frontal cortices, are impaired not only in phonological and word repetition but also in verbal short-term memory tasks (6, 7). Moreover, stimulation of the premotor cortex with repetitive transcranial magnetic stimulation disrupts the capacity to discriminate between phonemes (8). Similarly, learning new words is impaired if participants are engaged in the articulation of irrelevant sounds while they try to learn new ones (9). These studies are supportive of a link between auditory and motor processes in word learning.

Auditory and motor areas communicate directly through the AF, a pathway that shows a progressively high degree of complexity along the phylogenetic scale (10–13). Axonal tracing studies in monkey have shown that the AF connects to more dorsal regions of the temporo-parietal cortex (11, 14), whereas diffusion tensor imaging (DTI) studies in humans show a greater level of connectivity to auditory regions of the temporal lobe (10, 12). On the basis of these anatomical differences between human and other species, it has been suggested that the evolutionary expansion of auditory-motor connections allowed humans to develop a system for auditory working memory critical for learning complex phonological sequences (1, 15). There is, however, no

experimental evidence so far that links the anatomy of the AF with word learning ability.

In the current study, we aimed to seek direct evidence of the role of the AF in auditory-motor integration and word learning. For that, we explored the pattern of structural and functional connectivity between auditory and motor areas in both hemispheres as assessed by DTI-Tractography and fMRI while participants were learning words from fluent speech (Fig. 1A).

In our study we have used a recently described model of the AF (10, 16) in which communication between temporal and frontal language areas is mediated by two parallel networks: a direct pathway (i.e. the long segment of the AF) which connects the posterior part of both the superior (Brodmann Area [BA] 22) and the middle (BA 37) temporal gyrus (Wernicke's territory) and the inferior frontal gyrus (IFG, BA 44 and 45), middle frontal gyrus (BA 46) and premotor cortex (BA 6) (Broca's territory); and an indirect pathway composed of an anterior segment connecting Broca's territory with the inferior parietal cortex (IPL, BA 39 and 40) (Geschwind's territory) and a posterior segment connecting Geschwind's with Wernicke's territories (Fig. 1B). Our primary hypothesis was that word learning ability correlates with structural and functional connectivity of tracts directly connecting auditory and motor areas (i.e. long segment). Alternatively, previous evidence suggests that a ventral pathway running through the extreme capsule also connects the language areas (17–19). This path connects IFG (BA 45/47) with superior temporal gyrus [BA 22]), inferior parietal (BA 39) and occipital cortices (BA 17,18 and 19) (12, 18, 20) and it has been claimed to be important for spoken word recognition (21). During auditory word learning, the ventral pathway may allow the categorization of words as familiar once they have been learned, a point that could be also crucial for success. Therefore, the inferior fronto-occipital fasciculus (IFOF) was also bilaterally dissected (Fig. 1B and Fig. S1) in order to tease apart the possible contribution of the ventral pathway to word learning in its initial stages.

RESULTS

Virtual dissections of the AF and the IFOF were performed in 21 right-handed healthy subjects (mean age = 25.6 ± 3.9 years, 9 females) and surrogate measures of volume (i.e. number of

Reserved for Publication Footnotes

137
138
139
140
141
142
143
144
145
146
147
148
149
150
151
152
153
154
155
156
157
158
159
160
161
162
163
164
165
166
167
168
169
170
171
172
173
174
175
176
177
178
179
180
181
182
183
184
185
186
187
188
189
190
191
192
193
194
195
196
197
198
199
200
201
202
203
204

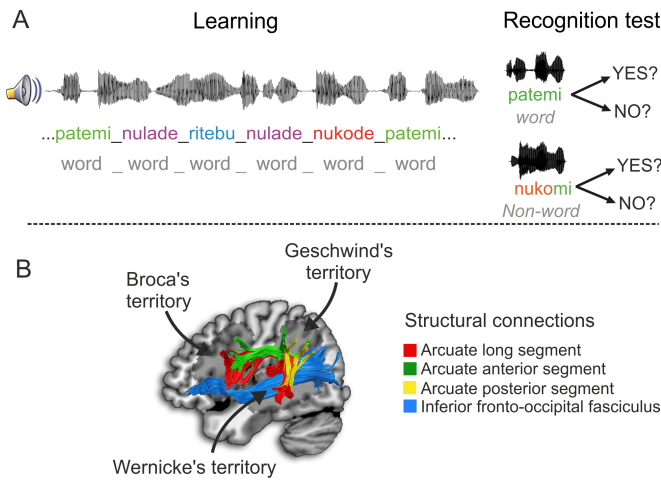


Fig. 1. Task and methods used in the study. **A.** Schematic illustration of the language-learning task used composed by a learning and a test phase. The learning phase consisted in the auditory presentation of an artificial language stream composed by trisyllabic words separated by subtle pauses. The test phase consisted in the presentation of isolated words (“words” or “non-words”) and participants were required to recognize each one as correct or incorrect based in the previously heard artificial language. **B.** Example of tractography reconstruction of language pathways in the left hemisphere for one of the subjects rendered onto the MNI template.

streamlines) and microstructural properties of fibers possibly related to the degree of myelination, axonal architecture and diameter (i.e. fractional anisotropy [FA] and radial diffusivity [RD]) were measured along reconstructed streamlines (22) (see Method). Analyses were performed separately for the three segments of the AF (Fig. 1B and SI Text) and the IFOF (Fig. 1B, Fig. S1 and SI Text) in both the left and right hemispheres.

The word-learning task involved two phases (Fig. 1A and Method). In the learning phase participants were asked to memorise artificially created words composed of three syllables presented in the form of a fluent speech stream (23). The words were novel to the participants and had no semantic content. The learning task was performed in the MRI scan during the fMRI experiment. Immediately after the learning phase, participants were behaviorally tested and asked to recognize auditory presented words (recognition phase) (see Method for further details). Word learning performances were measured using hit rates taking into account false alarms, calculating the d-prime (d') index (24), which reflects individual’s ability to discriminate words presented in the artificial language from non-presented words (non-words) (SI Text). One-sample t -test against $d' = 0$ (no discrimination) showed significant learning: $t(24) = 2.74, p < 0.01$.

Relationship between word learning performance and tract properties of the AF and the IFOF

AF. After Bonferroni’s correction for multiple comparisons, a statistically significant negative correlation was found between word learning performance and radial diffusivity ($r = -0.6; p < .005$) in the left long segment (Fig. 2; Table S1). Correlations with the anterior and posterior segments were not statistically significant (Fig. 2; and Table S1). There were no significant correlations with all three segments in the right hemisphere (Fig. 2; and Table S1). These findings suggest that microstructural properties of the dorsal direct connections between temporal and frontal language regions in the left hemisphere correlate with individual abilities to learn new words. In addition, a Lateralization Index (LI) was calculated by counting the number of reconstructed pathways within each segment of the AF for each hemisphere (see Method, SI Text and Fig. S2). In agreement with previous reports (16), the long segment showed a leftward lateralization, the anterior segment showed a rightward lateralization, while the posterior

segment showed a symmetrical distribution (Table S2 and Fig. S2). No significant correlation was observed between the LI of any of the segments of the AF and learning performance (Table S2).

IFOF. No statistically significant correlations were found between any of the DTI-derived measures and word learning scores for the IFOF of either hemisphere (Table S3). Lateralization analyses showed that the IFOF had a symmetrical distribution (Fig. S2 and Table S2). In addition, no significant correlation was observed between the LI of the IFOF and learning performance (Table S2).

Relationship between word learning performance and functional connectivity

Functional connectivity analyses were performed using the temporal correlation of the blood oxygen level-dependent (BOLD) response between the three regions of the perisylvian network connected by the direct and indirect segments of the AF on both hemispheres (see Method). Results showed that individual variations in the strength of the functional connectivity between the left temporal (Wernicke’s territory) and frontal (Broca’s territory) areas correlated with word learning performance ($r = 0.42, p < 0.036$; Figure 3A). The strength of connectivity between right frontal and temporal regions or between the regions connected by the indirect segments in both hemispheres was not significantly correlated with performance (all $p > 0.1$). In addition, laterality analyses of functional connectivity between regions connected by each AF segment were also calculated (see SI Text). The correlation between these functional connectivity LIs and word learning performance revealed no significant correlations (all $p > 0.09$; Table S4).

Relationship between structural and functional connectivity

Tract-specific measurements of single segments and strength of the functional connectivity between perisylvian areas were used to analyse possible correlations between anatomical and functional connectivity. We found no significant correlations between diffusion parameters and measures of functional connectivity (all $p > 0.1$).

DISCUSSION

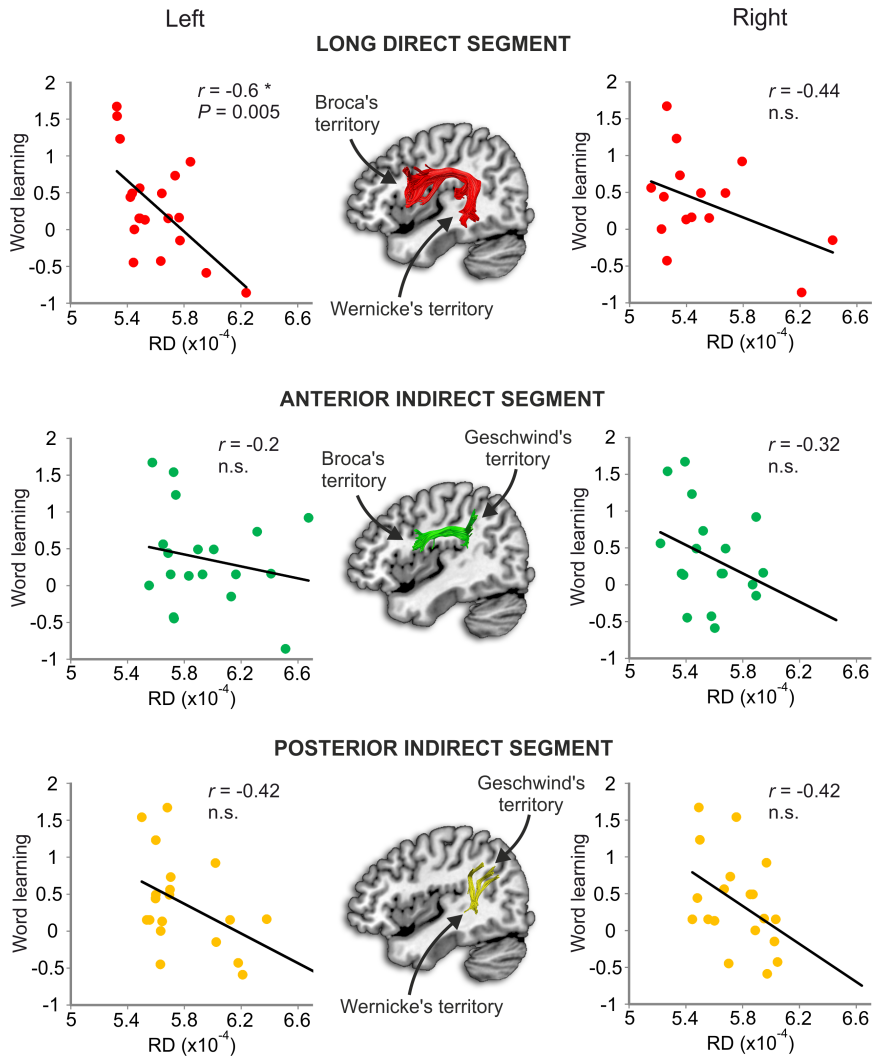
The present study combines tractography and fMRI in direct support of the role of the AF in word learning. Our main results suggest that both structural and functional measures of connectivity between temporal and frontal language territories in the left hemisphere predict word learning abilities. The fact that correlations for the indirect pathways were not significant suggests that the direct connections are crucial for audio-motor integration in word learning. The direct connections of the AF could mediate fast interaction between auditory and motor areas in the left hemisphere, thus facilitating those feed-forward and feed-back exchanges of information that are required to create motor codes of the new phonological sequences (4, 5). Moreover, this sensory-motor circuit may provide the substrate for articulatory-based processes that allow keeping information active during working memory (25, 26).

In addition, word learning did not correlate with any of the microstructural measures of the ventral IFOF, indicating that audio-motor integration through the dorsal pathway is the critical function at these earliest stages of language learning. The ventral pathway may nevertheless play a greater role at later stages of learning, when auditory representations of learned words are consolidated by taking into account invariance properties after multiple encounters (27) as well as once conceptual representations have been attached to the new-words learned (28).

A basic aspect of human language is its left-side lateralization (29). In our study, the correlation between language learning and the AF direct segment was exclusively found in the left hemisphere. This left lateralized relation was not relative to the charac-

205
206
207
208
209
210
211
212
213
214
215
216
217
218
219
220
221
222
223
224
225
226
227
228
229
230
231
232
233
234
235
236
237
238
239
240
241
242
243
244
245
246
247
248
249
250
251
252
253
254
255
256
257
258
259
260
261
262
263
264
265
266
267
268
269
270
271
272

273
274
275
276
277
278
279
280
281
282
283
284
285
286
287
288
289
290
291
292
293
294
295
296
297
298
299
300
301
302
303
304
305
306
307
308
309
310
311
312
313
314
315
316
317
318
319
320
321
322
323
324
325
326
327
328
329
330
331
332
333
334
335
336
337
338
339
340



PDF

Fig. 2. Link between the microstructure of the arcuate fasciculus and word learning performance. The scatter plots show the correlations between word learning scores (d-prime [d']) and radial diffusivity (RD) in the long, the anterior and the posterior segments of the arcuate fasciculus for the left and right hemispheres. The index of correlation and the p-value are provided on each plot box. "*" indicates the significant correlation ($p < 0.0062$). Non-significant correlations are marked as "n.s." $d' = 0$ designates no learning. Positive values reflect that participants discriminate words and non-words accurately. Negative values indicate discrimination is achieved but individuals segmented incorrectly, classifying non-words as words of the artificial language.

341
342
343
344
345
346
347
348
349
350
351
352
353
354
355
356
357
358
359
360
361
362
363
364
365
366
367
368
369
370
371
372
373
374
375
376
377
378
379
380
381
382
383
384
385
386
387
388
389
390
391
392
393
394
395
396
397
398
399
400
401
402
403
404
405
406
407
408

teristics of the right AF because lateralization indexes showed no correlation to word-learning performance. Previous work found correlations between verbal memory for known words and the AF bilaterally (16). The lateralization difference compared to our study can be related to the use of a semantic recall strategy for real words which is associated to bilateral activation of fronto-temporal networks (30). In contrast, no semantic component was present in our task, designed to have a purely phonological component and therefore more likely to rely on a more simple audio-motor integration strategy.

The present findings add novel insights into the relationship between brain morphology and language proficiency, previously explored by neuroimaging studies looking at the anatomy of single cortical regions. For example, the grey matter density of Broca's area has been found to correlate with the level of language proficiency (31) and the number of years of phonetic training in expert phoneticians (32). Similarly, white matter density in left parietal regions (33, 34) and the superior temporal gyrus (34) predicts speech sound learning. Interestingly, a recent study has shown that changes in the cortical thickness of Broca's area and left superior temporal gyrus can occur even only after three months of intensive language training (35). On the other hand, the aforementioned findings, together with our results, contrast with retrospective studies showing an association between grey matter density in the posterior parietal cortex and vocabulary

size of the first (36) and second language (37). This suggests that learning and storing new words rely on different anatomical structures, the former on temporal-frontal regions, the latter on inferior parietal areas.

The correlation we found with structural measures of connectivity suggests that radial diffusivity is a sensitive index of white matter microstructural features underlying efficient cognitive processing. Several factors like axon diameter, packing density, fiber crossing, number of axons, myelination of axons and myelin thickness may contribute to radial diffusivity signal (22). Importantly, thicker myelin and larger diameter axons are correlated with increased conduction of action potentials through long association fibers (38). A decrease in radial diffusivity, i.e. the average of the diffusivities along the two minor axes of the tensor model (39), is likely to reflect increased myelination or increased axonal diameter (40). Hence, the correlation reported in our study suggests that a possible explanation for the interindividual variability in word learning is due to differences in the anatomy of direct connections between left auditory and motor areas. One could speculate that fibers with larger axons and/or greater myelination facilitate faster conduction of impulses leading to better synchronization and information transfer between distant regions.

In addition, our results show that functional connectivity is an independent predictor of word learning performance. Several

409
410
411
412
413
414
415
416
417
418
419
420
421
422
423
424
425
426
427
428
429
430
431
432
433
434
435
436
437
438
439
440
441
442
443
444
445
446
447
448
449
450
451
452
453
454
455
456
457
458
459
460
461
462
463
464
465
466
467
468
469
470
471
472
473
474
475
476

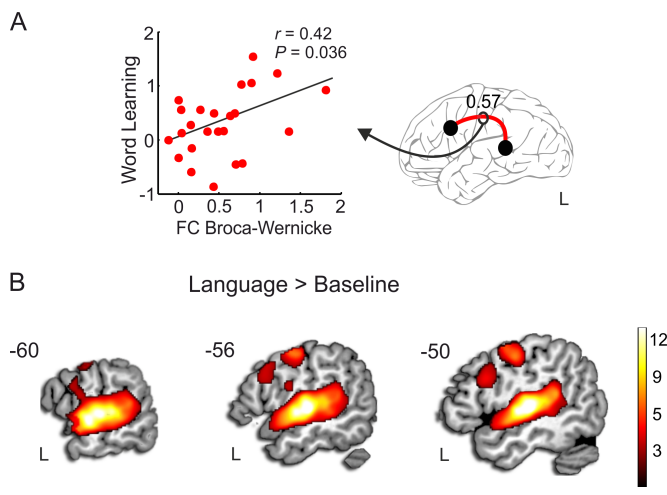


Fig. 3. Functional MRI analyses. A. Scatter plot showing the correlation between word learning (d') and the amount of functional connectivity between Broca's and Wernicke's territories in the left hemisphere during the word learning task. Correlation index and the p-value are provided on the plot box. The averaged functional connectivity (significantly different from zero, $p < 0.001$) is also shown. B. Language versus rest contrast in sagittal views superimposed on the MNI template ($p < 0.05$ FDR corrected). Only activations in the left hemisphere are shown in the figure. See Table S5 for peak activation coordinates.

studies have focused on the physiological processes underpinning the fluctuations that are commonly observed in the BOLD response as measured by fMRI (41–43). The BOLD signal is sensitive to changes in the oxygenation of the blood in a given area, thus associated to its increased neuronal activation (44). In relation to neural activity, BOLD response fluctuations reflects more the input and local processing of an area rather than its output (i.e., spiking activity) (43). Conversely, DTI is more sensitive to differences in white matter microstructure, such as axonal density, myelination or fiber diameter (22). These microstructural properties of fibers are likely to facilitate a faster signal conduction but they may not be related to integrative processes performed at the cortical level (45, 46). Indeed, our results suggest that, although both functional and anatomical measures of connectivity are correlated to language learning performances, a correlation between them should not be assumed.

Crucially, the AF, taken as a possible anatomical substrate of audio-motor integration, might represent a key step for language development. Comparative studies indicate that apes and monkeys have homologues for Broca's and Wernicke's areas in terms of grey matter (47, 48) and both dorsal and ventral connections between them (47). However, the trajectory of the AF is different between species. Middle and inferior temporal gyri terminations from the inferior frontal gyrus are more prominent in humans than in macaques and chimpanzees (12, 13, 47). In addition, the AF appears to show a greater modification in human evolution than the ventral extreme fiber system (49). Indeed, while humans and chimpanzees show a dominant connection between Broca's and Wernicke's territories through the AF, macaques show a predominant connection through the ventral pathway (13). This latter path, involved in auditory object identification is the one processing calls and vocalizations in these lower species (49). Interestingly, monkeys, that have a smaller AF compared to humans (11, 14), are able to perform complex tactile and visual memory tests but these skills are lost in the auditory modality (50). This suggests that the ability to integrate audio-motor information confers some advantages in the manipulation of the representation of acoustic stimuli, thus allowing its storage in the long-term memory.

Ontogenetically, the AF develops slower than other associative pathways, including the ventral pathway (19). Its terminations connecting with Broca's area show progressive development during childhood, still under development at the age of 7 (51, 52). However the connections with premotor cortex, those responsible to audio-motor integration, can be tracked in newborns (19, 52), suggesting a role in early language acquisition. Very early pre-linguistic damage to the AF (53) induces delayed expressive language development and residual language difficulties remain even when within normal levels of expressive language are reached later on through the available connectivity of the ventral pathway. Similar lesions after the age of 5 (54) lead to preserved oral language, although with poor performance in nonword repetition, verbal working memory and reading. In healthy adults, the use of articulatory suppression to block the use of the dorsal pathway interferes with word learning also, and performance under this condition correlates with the individual differences in the microstructural properties of the ventral pathway (9). Taken together, the above studies indicate that lesions to the AF induce language-learning difficulties. Even when the ventral system can compensate for language learning, optimal performance cannot be reached after complete damage of the AF.

It is noteworthy that in spite of the differences in terminology, each of the three segments composing the AF in the model followed in the current study correspond to what has been previously described for the monkey brain (11, 12). The anterior segment corresponds to the third superior longitudinal fasciculus bundle (SLF III); the long segment corresponds specifically to the arcuate *sensu strictu*; and the posterior segment corresponds to the middle longitudinal fasciculus. In this study we have used DTI instead of more advanced methods such as High Angular Resolution Diffusion Imaging or diffusion spectral imaging [HARDI]/DSI). These methods lead to greater number of false positives streamlines in the AF reconstruction that need to be anatomically validated (55). Thus for AF tractography, DTI remains a more conservative and reliable method nowadays (for a more in depth critique, see (56)).

In conclusion, the present results support the idea that the direct segment of the AF is crucial for word learning, most probably due to its relevance for proper audio-motor integration. This study also sheds light on the origin of the large individual variability observed when learning a new language and gives support to the idea that anatomical brain connectivity constrains the nature of the information processed across brain regions (57). Finally, the big differences existing between humans and non-human primates in language learning might be related to the evolution of the AF, a pathway that has been shown to be structurally different in non-human primates, and that allows the processing and manipulation of complex auditory information.

MATERIALS AND METHODS

Participants

Twenty-seven participants (mean age = 24.7 ± 4.6, 12 women) were recruited for the experiment. Participants were native Spanish speakers with no history of auditory problems. All participants in this study were considered right handed after completing the Edinburgh Handedness Inventory (mean 80.4 ± 20.4)(58). The ethical committee of the University of Barcelona approved the protocol and written consent was obtained from all participants. Participants were paid for their participation. Six participants were removed for the tractography analyses due to MRI acquisition problems and two participants were removed from the behavioural correlations because no behavioural data was obtained from them. The final sample resulted in 20 subjects for the behavioral-tractography correlations, 25 for the behavioral-functional connectivity correlation and 21 for the tractography-functional correlations.

Language learning task-design

An artificial language learning task was administered into the scanner (Fig. 1A) through two runs. Eight different languages were built with each participant listening to two different languages. Languages were counter-balanced between subjects and were built by creating words composed of three syllables. Words were synthesized using the MBROLA speech syn-

477
478
479
480
481
482
483
484
485
486
487
488
489
490
491
492
493
494
495
496
497
498
499
500
501
502
503
504
505
506
507
508
509
510
511
512
513
514
515
516
517
518
519
520
521
522
523
524
525
526
527
528
529
530
531
532
533
534
535
536
537
538
539
540
541
542
543
544

thesizer software (59) concatenating diphones at 16 kHz from the Spanish male database (tcts.fpms.ac.be/synthesis/mbrola.html). Languages were composed by 9 different novel words built following Spanish phonotactic constraints. Each word had a 696 msec duration and subtle pauses of 25 msec were inserted between them in order to introduce a prosodic cue to mark words boundaries (60). Words were presented in pseudorandom order (i.e. the same word was not repeated in succession) and in the form of a fluent speech stream. The material was similar to the one used in De Diego-Balaguer et al (23).

The task involved a *learning* phase and a *test* phase (Fig. 1A). During the *learning phase*, four active blocks lasting 30 seconds, including 42 word presentations each were presented. Active blocks were alternated with resting blocks of 20 seconds duration where participants were asked to simply fixate their gaze on a cross that remained in the middle of the screen.

Participants were told that they would hear a nonsense language and that their task was to pay attention because they would be asked to recognize words of this language after the listening. Immediately after the learning phase, participants were behaviorally tested (*recognition phase*). Isolated words were presented auditory and participants were required to judge whether each word had appeared in the previously learned language stream. The words presented in the test could be previously presented words, or non-words, formed with the same three syllables of a previously exposed word in an incorrect order (Fig. 1A). Each test item appeared three times in each recognition phase leading to 36 test trials. Responses were recorded using an MR-compatible response box containing two response keys (forefinger and middle-finger). Participants were required to press the left button if they judged the item to be a word presented before and the right button if not. The experiment was run using the Presentation Software (<http://nbs.neuro-bs.com/>). Stimuli were played through MR-compatible headphones.

MRI acquisition

Images were acquired on a 3-T MRI scanner (Siemens Magnetom Trio) with 40-mT/m gradients, using an acquisition sequence fully optimized for DT-MRI of white matter, with the following parameters: voxel size of 2.0 x 2.0 x 2.0 mm, matrix 128 x 128, 64 slices with 2 mm-thick and no gap, NEX 1, TE 88 ms, b-value 1000 s/mm², 8 runs of 12 diffusion-weighted directions and 7 non-diffusion-weighted volumes, using a spin-echo EPI sequence coverage of the whole head. DTI images were acquired before the fMRI sequence. High-resolution structural images (T1-weighted sequence: slice thickness = 1mm; no gap; number of slices = 240; repetition time (TR) = 2300ms; echo time (TE) = 3ms; matrix = 256 x 256; field of view FOV = 244 mm) were also acquired. Subsequently, functional images were obtained by using a single-shot T2*-weighted gradient-echo EPI sequence (slice thickness = 4mm; no gap; number of slices = 32, order of acquisition interleaved; repetition time (TR) = 2000 ms; echo time (TE) = 29 ms; flip angle = 80°; matrix = 128 x 128; field of view FOV = 240 mm).

DTI-MRI Tractography

Preprocessing of DTI data

Diffusion data was processed using Explore DTI (<http://www.exploredti.com>). Data was first pre-processed correcting for eddy current distortions and head motion. For each subject the b-matrix was then reoriented to provide a more accurate estimate of diffusion tensor orientations (61). Remaining artefacts due to subject motion and cardiac pulsation were excluded from the analysis using the RESTORE (62) to reject and correct outliers from diffusion-weighted imaging (DWI) data. Diffusion tensor was estimated using a non linear least square approach (63) and Fractional Anisotropy (FA) and Radial Diffusivity (RD) maps were calculated. Whole brain tractography was performed using a b-spline interpolation of the DT field and Euler integration to propagate streamlines following the directions of the principal eigenvector with a step size of 0.5 mm (64). Tractography was started in all brain voxels with FA > 0.2. Tractography was stopped where FA < 0.2 or when the angle between two consecutive tractography steps was larger than 35 degrees. This whole-brain approach ensures that tractography reconstruction is not dependent on the ROI delineation. Finally, tractography data and diffusion tensor maps were exported to Trackvis (65) for manual dissection of the tracts.

Tractography dissections

Virtual dissections of the AF and the IFOF were carried out as previous studies have described (10, 16, 66)(see SI Text for further details). Dissections were performed for each subject in the native space and in both hemispheres. The color fiber orientation maps were resliced in axial, coronal, and sagittal planes and displayed in conjunction with tractography results to allow an approximation to the neuroanatomical location of the tract reconstructions. Because brain regions may have significant interindividual differences, regions of interest (ROIs) were manually defined (i.e., the dissec-

tor placed the ROI according individual anatomical landmarks, rather than coordinates or atlas-based constraints that may not apply to each single subject). The approach does not constrain tracts to start and end within the defined regions, only to pass through them (SI Text).

Fiber Track measures

Number of streamlines (Ns), fractional anisotropy (FA) and radial diffusivity (RD) were extracted and averaged along each of the entire tracks segmented (22). Number of streamlines is considered a surrogate measure of tract volume; FA is considered a measure linked to axon packing and myelination; RD described microscopic water movements perpendicular to the axons tracks (67) and it has been postulated to reflect myelin quality along the axon. Demyelination (68) as well clinical disability and severe tissue injury (69) has been associated with increased RD.

Statistical analysis

The statistical analysis was performed using the SPSS software. Pearson's correlation analyses were performed between the learning performance (d-prime index) and the DTI measures (Ns, FA, RD) along each segment (long, anterior, posterior) of the AF as well as for the IFOF pathway from both hemispheres (Fig. 1B). Correlations were considered significant at $p < 0.0062$ after Bonferroni's correction for multiple comparisons. Values that were greater than two standard deviations from the mean were considered outliers and were removed from the analyses (see Tables S1 and S3 for the final sample of each correlation analysis). A lateralization index (LI) was calculated for both the number of streamlines and FA according to the following formula: ((left)-(right)) / ((left)+(right)) (SI Text)(16).

Functional-MRI

Preprocessing

Data were preprocessed using Statistical Parameter Mapping software (SPM8, Wellcome Department of Imaging Neuroscience, University College, London, UK, www.fil.ion.ucl.ac.uk/spm/). Preprocessing included realignment, coregistration between the mean functional and the structural T1, segmentation, normalization and smoothing with a 8 mm FWHM Gaussian kernel. Normalization was performed using DARTEL (70).

Statistical analysis was based on a least-square estimation using the general linear model by convolving a box-car regressor waveform with a canonical hemodynamic response function. Two main conditions of interest were modeled, language and rest. Parameters from head movement, obtained from realignment, were also included in the model. Main effects for each condition were calculated and the contrast of interest (language versus rest) was estimated for each participant. A second level RFX analysis was performed by using a one-sample t-test on the main contrast derived from the single subject data. Results are shown at a $p < 0.05$ FDR corrected (see Fig. 3B; and Table S5).

Functional connectivity (fcMRI) and statistical analysis

Three ROIs were manually defined based on the anatomical gyri around the territories connected by the direct and the indirect segments of the AF (SI Text; and Fig. S3). First level subject specific Language vs. rest contrasts were masked with the defined ROIs, and for each subject, the peak coordinate within each ROI was selected. Eight-millimeter radius 3D-seeds were placed at the selected coordinates and mean voxel time course series was extracted. These mean time courses were low-pass filtered and had the linear trend removed. MATLAB toolbox for functional connectivity (71) includes a function to calculate the relationship between two regions, after taking into account the influence of any other area. This toolbox was used to calculate correlations between the time series of each pair of territories. Finally, this calculated correlation was transformed to a normal distribution using Fischer's z transform (72).

Functional-behavioral correlations were calculated for the areas in the frontal, temporal and parietal cortices that the direct and the indirect segments of the AF connect (Broca, Wernicke and Geschwind territories, respectively). Each subject's z-transformed left and right correlations were regressed with behavioral performance (d-prime scores).

ACKNOWLEDGEMENTS.

The authors wish to thank Virginia Penhune for her helpful discussions on the results. The present project has been funded by the Spanish Government (MINECO Grants to R.D.B, PSI2011-23624 and to A.R.F., PSI2011-29219). D.L.B. has been supported by a predoctoral grant (2010FI.B1 00169) from the Catalan government. P.R has been supported by a predoctoral grant from the Spanish Government (FPU program AP2010-4179). This study was in part supported by Guy's and St Thomas' Charity (GSST) and the Biomedical Research Centre for Mental Health at South London and Maudsley NHS Foundation Trust and Institute of Psychiatry, King's College London.

1. Schulze K, Vargha-Khadem F, Mishkin M (2012) Test of a motor theory of long-term auditory memory. *Proc Natl Acad Sci U S A* 109:7121–5.
2. Liberman AM, Mattingly IG (1985) The motor theory of speech perception revised. *Cognition* 21:1–36.
3. Hickok G, Poeppel D (2007) The cortical organization of speech processing. *Nat Rev Neurosci* 8:393–402.
4. Rauschecker JP, Scott SK (2009) Maps and streams in the auditory cortex: nonhuman primates illuminate human speech processing. *Nat Neurosci* 12:718–24.

5. Rodríguez-Fornells A, Cunillera T, Mestres-Missé A, de Diego-Balaguer R (2009) Neurophysiological mechanisms involved in language learning in adults. *Philos Trans R Soc Lond B Biol Sci* 364:3711–3735.
6. Benson D et al. (1973) Conduction aphasia: a clinicopathological study. *Archives of Neurology* 28:339–346.
7. Damasio H, Damasio A (1980) The anatomical basis of conduction aphasia. *Brain* 103:337–350.
8. Meister IG, Wilson SM, Deblieck C, Wu AD, Iacoboni M (2007) The essential role of

681 premotor cortex in speech perception. *Curr Biol* 17:1692–6.

682 9. Lopez-Barroso D et al. (2011) Language learning under working memory constraints

683 correlates with microstructural differences in the ventral language pathway. *Cereb Cortex*

684 21:2742–2750.

685 10. Catani M, Jones DK, Ffytche DH (2005) Perisylvian language networks of the human brain.

686 *Ann Neurol* 57:8–16.

687 11. Schmahmann JD et al. (2007) Association fibre pathways of the brain: parallel observations

688 from diffusion spectrum imaging and autoradiography. *Brain* 130:630–53.

689 12. Thiebaut de Schotten M, Dell'Acqua F, Valabregue R, Catani M (2012) Monkey to human

690 comparative anatomy of the frontal lobe association tracts. *Cortex* 48:82–96.

691 13. Rilling JK et al. (2008) The evolution of the arcuate fasciculus revealed with comparative

692 DTI. *Nat Neurosci* 11:426–8.

693 14. Petrides M, Pandya D (1984) Projections to the frontal cortex from the posterior parietal

694 region in the rhesus monkey. *Journal of Comparative Neurology* 228:105–116.

695 15. Aboitiz F (2012) Gestures, vocalizations, and memory in language origins. *Front Evol Neurosci*

696 4:2.

697 16. Catani M et al. (2007) Symmetries in human brain language pathways correlate with verbal

698 recall. *Proc Natl Acad Sci U S A* 104:17163–8.

699 17. Saur D et al. (2008) Ventral and dorsal pathways for language. *Proc Natl Acad Sci U S A*

700 105:18035–18040.

701 18. Martino J et al. (2011) Cortex-sparing fiber dissection: an improved method for the study of

702 white matter anatomy in the human brain. *J Anat* 219:531–41.

703 19. Saccuman MC et al. (2011) Neural language networks at birth. *Proceedings of the National*

704 *Academy of Sciences* 108:18566–18566.

705 20. Catani M, Howard RJ, Pajevic S, Jones DK (2002) Virtual in Vivo Interactive Dissection of

706 White Matter Fasciculi in the Human Brain. *Neuroimage* 17:77–94.

707 21. DeWitt I, Rauschecker JP (2012) Phoneme and word recognition in the auditory ventral

708 stream. *Proc Natl Acad Sci U S A* 109:E505–14.

709 22. Beaulieu C (2002) The basis of anisotropic water diffusion in the nervous system - a technical

710 review. *NMR Biomed* 15:435–455.

711 23. De Diego-Balaguer R, Toro JM, Rodríguez-Fornells A, Bachoud-Lévi A-C (2007) Different

712 neurophysiological mechanisms underlying word and rule extraction from speech. *PLoS One*

713 2:e1175.

714 24. MacMillan N, Creelman C (2005) *Detection Theory: A User's Guide*. (Lawrence Erlbaum

715 Associated, Publishers)Second Edi.

716 25. Buchsbaum BR, D'Esposito M (2008) The search for the phonological store: from loop to

717 convolution. *J Cogn Neurosci* 20:762–78.

718 26. Cunillera T et al. (2009) Time course and functional neuroanatomy of speech segmentation

719 in adults. *Neuroimage* 48:541–53.

720 27. Romanski LM, Tian B, Fritz J, Mishkin M, Rauschecker JP (1999) Dual streams of auditory

721 afferents target multiple domains in the primate prefrontal cortex. 1131–1136.

722 28. Mestres-Missé A, Càmara E, Rodríguez-Fornells A, Rotte M, Münte TF (2008) Functional

723 neuroanatomy of meaning acquisition from context. *J Cogn Neurosci*:2153–2166.

724 29. Geschwind N (1970) The organization of language and the brain. *Science (80-)* 170:940–944.

725 30. Johnson S, Saykin A, Flashman L, McAllister T, Sparling M (2001) Brain activation on fMRI

726 and verbal memory ability: functional neuroanatomic correlates of CVLT performance. *J Int*

727 *Neuropsychol Soc* 7:55–62.

728 31. Stein M et al. (2012) Structural plasticity in the language system related to increased second

729 language proficiency. *Cortex* 48:458–65.

730 32. Golestani N, Price CJ, Scott SK (2011) Born with an ear for dialects? Structural plasticity in

731 the expert phonetician brain. *J Neurosci* 31:4213–20.

732 33. Golestani N, Paus T, Zatorre RJ (2002) Anatomical correlates of learning novel speech

733 sounds. *Neuron* 35:997–1010.

734 34. Golestani N, Molko N, Dehaene S, LeBihan D, Pallier C (2007) Brain structure predicts the

735 learning of foreign speech sounds. *Cereb Cortex* 17:575–82.

736 35. Mårtensson J et al. (2012) Growth of language-related brain areas after foreign language

737 learning. *Neuroimage* 63:240–4.

738 36. Lee H et al. (2007) Anatomical traces of vocabulary acquisition in the adolescent brain. *J*

739 *Neurosci* 27:1184–9.

740 37. Mechelli A et al. (2004) Structural Plasticity in the bilingual brain. *Nature* 431:757.

741 38. Fields RD (2008) White matter in learning, cognition and psychiatric disorders. *Trends*

742 *Neurosci* 31:361–70.

743 39. Beaulieu C (2010) in *Diffusion MRI*, ed Jones DK (Oxford University Press, New York), pp

744 92–109.

745 40. Song S-K et al. (2002) Dysmyelination Revealed through MRI as Increased Radial (but

746 Unchanged Axial) Diffusion of Water. *Neuroimage* 17:1429–1436.

747 41. Ogawa S, Lee T (1990) Magnetic resonance imaging of blood vessels at high fields: in vivo

748 and in vitro measurements and image simulation. *Magnetic resonance in medicine* 16:9–18.

749 42. Kwong K et al. (1992) Dynamic magnetic resonance imaging of human brain activity during

750 primary sensory stimulation. *Proc Natl Acad Sci U S A* 89:5675–5679.

751 43. Logothetis NK, Pauls J, Augath M, Trinath T, Oeltermann a (2001) Neurophysiological

752 investigation of the basis of the fMRI signal. *Nature* 412:150–7.

753 44. Ogawa S, Lee T, Nayak A, Glynn P (1990) Oxygenation-sensitive contrast in magnetic

754 resonance image of rodent brain at high magnetic fields. *Magnetic resonance in medicine*

755 14:68–78.

756 45. Demerens C et al. (1996) Induction of myelination in the central nervous system by electrical

757 activity. *Proc Natl Acad Sci U S A* 93:9887–92.

758 46. Zatorre RJ, Fields RD, Johansen-Berg H (2012) Plasticity in gray and white: neuroimaging

759 changes in brain structure during learning. *Nat Neurosci* 15:528–36.

760 47. Petrides M, Pandya DN (2009) Distinct parietal and temporal pathways to the homologues

761 of Broca's area in the monkey. *PLoS Biol* 7:e1000170.

762 48. Schenker NM et al. (2008) A comparative quantitative analysis of cytoarchitecture and

763 minicolumnar organization in Broca's area in humans and great apes. *J Comp Neurol*

764 510:117–28.

765 49. Rilling JK, Glasser MF, Jbabdi S, Andersson J, Preuss TM (2011) Continuity, divergence, and

766 the evolution of brain language pathways. *Front Evol Neurosci* 3:11.

767 50. Fritz J, Mishkin M, Saunders RC (2005) In search of an auditory engram. *Proc Natl Acad Sci*

768 *U S A* 102:9359–64.

769 51. Brauer J, Anwender A, Friederici AD (2011) Neuroanatomical prerequisites for language

770 functions in the maturing brain. *Cereb Cortex* 21:459–66.

771 52. Brauer J, Anwender A, Perani D, Friederici AD (2013) Dorsal and ventral pathways in

772 language development. *Brain & Language* (in press):1–7.

773 53. Yeatman JD, Feldman HM (2013) Neural plasticity after pre-linguistic injury to the arcuate

774 and superior longitudinal fasciculi. *Cortex* 49:301–11.

775 54. Rauschecker AM et al. (2009) Reading impairment in a patient with missing arcuate

776 fasciculus. *Neuropsychologia* 47:180–94.

777 55. Dell'Acqua F, Catani M (2012) Structural human brain networks: hot topics in diffusion

778 tractography. *Curr Opin Neurol* 25:375–83.

779 56. Catani M et al (in press) Connectomic approaches before the connectome. *Neuroimage*.

780 57. Johansen-Berg H (2007) Structural Plasticity: Rewiring the Brain. *Current Biology*

781 17:R141–R144.

782 58. Oldfield R (1971) The assessment and analysis of handedness: the Edinburgh inventory.

783 *Neuropsychologia* 9:97–113.

784 59. Dutoit T, Pagel V, Pierret N, Bataille F, Vreken O (1996) in *Proceedings of ICSLP*.

785 60. Peña M, Bonatti LL, Nespor M, Mehler J (2002) Signal-Driven Computations in Speech

786 Processing. *Science (80-)* 298:604–607.

787 61. Leemans A, Jones DK (2009) The B-matrix must be rotated when correcting for subject

788 motion in DTI data. *Magn Reson Med* 61:1336–49.

789 62. Chang L-C, Jones DK, Pierpaoli C (2005) RESTORE: robust estimation of tensors by outlier

790 rejection. *Magn Reson Med* 53:1088–95.

791 63. Jones DK, Basser PJ (2004) "Squashing peanuts and smashing pumpkins": how noise distorts

792 diffusion-weighted MR data. *Magn Reson Med* 52:979–93.

793 64. Basser PJ, Pajevic S, Pierpaoli C, Duda J, Aldroubi a (2000) In vivo fiber tractography using

794 DT-MRI data. *Magn Reson Med* 44:625–32.

795 65. Wang R, Benner T, Sorensen A, Wedeen V (2007) in *Proceedings of the International Society*

796 *for Magnetic Resonance in Medicine*, p 3720.

797 66. Catani M, Thiebaut de Schotten M (2008) A diffusion tensor imaging tractography atlas for

798 virtual in vivo dissections. *Cortex* 44:1105–1132.

799 67. Klawiter EC et al. (2011) Radial diffusivity predicts demyelination in ex vivo multiple sclerosis

800 spinal cords. *Neuroimage* 55:1454–60.

801 68. Song S-K et al. (2002) Dysmyelination Revealed through MRI as Increased Radial (but

802 Unchanged Axial) Diffusion of Water. *Neuroimage* 17:1429–1436.

803 69. Naismith RT et al. (2010) Radial diffusivity in remote optic neuritis discriminates visual

804 outcomes. *Neurology* 74:1702–10.

805 70. Ashburner J (2007) A fast diffeomorphic image registration algorithm. *Neuroimage*

806 38:95–113.

807 71. Zhou D, Thompson W, Siegle G (2009) MATLAB toolbox for functional connectivity.

808 *Neuroimage* 47:1590–1607.

809 72. Barber AD et al. (2012) Motor "dexterity": Evidence that left hemisphere lateralization of

810 motor circuit connectivity is associated with better motor performance in children. *Cereb*

811 *Cortex* 22:51–9.